Order and Defects of Langmuir-Blodgett Films Detected with the Atomic Force Microscope

Jouko P. K. Peltonen,* Pingsheng He,† and Jarl B. Rosenholm

Contribution from the Department of Physical Chemistry, Åbo Akademi University, Porthansgatan 3-5, SF-20500 Turku, Finland. *Received April 6, 1992*

Abstract: The atomic force microscope (AFM) has been used to image multilayer Langmuir-Blodgett (LB) films of *trans*-6-octadecenoic acid deposited on an amorphous glass plate. The two-dimensional fast fourier transform analysis of the AFM image together with the consecutive inverse transform is suggested for obtaining the salient structural packing features of the LB films. Well-ordered periodic structures with molecular resolution could be obtained by using a cantilever with a spring constant of 0.38 N/m. Several dislocations were found on areas typically of the size 100 × 100 nm^2. Line profiles revealed the existence of density fluctuations in the film most probably arising from the electrostatic interactions present in the polar head group region. The LB films studied showed the characteristics of liquid crystalline phases with a packing symmetry varying with the counterion used.

Introduction

The increasing interest toward technical applications of Langmuir-Blodgett (LB) films emphasizes the need to pay special attention on the mechanical stability of the film structures. Polymerizable surface active substances offer an interesting alternative to produce extremely stable thin and homogeneous organic films. We have hence investigated the conditions needed to produce nanometer thick films formed by unsaturated fatty acids.[1,2] In this report we emphasize the topographical properties of *trans*-6-octadecenoic acid monomer LB films. We present molecularly resolved AFM images of LB films deposited on amorphous glass slides. Comparisons between the surface characteristics of the pure glass substrate and those covered with mono- and multilayer LB films will be made. Different types of dislocations interrupting the otherwise well-ordered multilayer structure will be presented. The difference in monolayer packing when using either $CdCl_2$ or $TbCl_3$ subphase will be shown.

The atomic force microscope (AFM)[3] is a new tool for surface imaging which was introduced as one application of the scanning tunneling microscope (STM).[4] Among many applications, due to its extreme resolution the AFM has been used to image organic samples including LB films.[5-13] These films are most often insulating and soft and are thus difficult to image. As compared with the STM, the AFM can provide important advantages since no surface conductivity on the substrate is needed to get an AFM image and it is thus independent of the charge transfer between the sample and the tip. Operated with small contact forces between the tip and the sample as well as equipped with the state-of-the-art *xyz*-piezoscanners the instrument reports on surface topology without damaging or modifying the surface.[10-12] In this report we have paid special attention on the choice of cantilever as well as the force minimization between the cantilever and the surface under study. After testing four types of cantilevers with different spring constants, we reached the best resolution by using a cantilever with a spring constant of 0.38 N/m. We have also taken great advantage of the determination of the two-dimensional fast fourier transform (FFT) of the AFM image in obtaining the crystal parameters as well as the filtered inverse-transformed image.

Experimental Section

LB Film Preparation. A well-known LB technique[14] was used to prepare the samples. *trans*-6-Octadecenoic acid (TODA) was used as the film-forming material. The surfactant of 99% purity was supplied by Sigma Corp. and used without further purification. The surfactant was dissolved in hexane to form a solution of 1 mg/mL. Until spread on either 10^{-4} M $CdCl_2$ or $TbCl_3$ subphase, the solution was protected against light and stored in a freezer. The Langmuir-Blodgett films were prepared by using a KSV-5000 film deposition system (KSV-Instruments, Helsinki, Finland) under a constant subphase pH of 5.8 ± 0.2 and at a temperature of 20° ± 0.3 °C controlled with a thermostated trough. The surface pressure was monitored with a Pt-Wilhelmy plate. The water used as the subphase was purified with the Milli Q filtration system (Millipore Corp., USA) to give water resistances as high as 18 MΩ cm. The lipid molecules were spread on the subphase surface with a microsyringe. To enable the hexane to evaporate completely, the compression was started 10-15 min after spreading. The compression rate (the barrier speed) used was 10 mm/min and the compression was continued until the pre-set deposition surface pressure was reached. The Langmuir film was transferred to an amorphous glass plate at a surface pressure kept constant with a computer-driven feedback system. In the primary layer the polar head groups are oriented toward the glass substrate and the hydrocarbon chains are oriented toward air. A continued deposition hence resulted in a Y-type multilayer structure.[15] The deposition was started after a stabilization period of 15 min. A dipping speed of 10 mm/min was used. Before deposition, the glass plates were soaked in a chromic acid mixture of 1-2 days followed by a NaOH-alcohol bath of several hours. They were finally dried in air flow prior to use. The

* Author to whom correspondence should be addressed.
† On leave from The University of Science and Technology of China, Hefei 230026, Anhui, People's Republic of China.

(1) Peltonen, J. P. K.; Rosenholm, J. B. *Thin Solid Films* **1989**, *179*, 543-547.
(2) Peltonen, J. P. K.; Linden, M.; Rosenholm, J. B. *Proceedings of the FEBS Satellite Meeting*, 1990, p 63.
(3) Binnig, G.; Quate, C. F.; Gerber, Ch. *Phys. Rev. Lett.* **1986**, *56*, 930-933.
(4) Binnig, G.; Rohrer, H.; Gerber, Ch.; Weibel, E. *Phys. Rev. Lett.* **1982**, *49*, 57-61.
(5) Gould, S.; Marti, O.; Drake, B.; Hellemans, L.; Bracker, C. E.; Hansma, P. K.; Keder, N. L.; Eddy, M. M.; Stucky, G. D. *Nature* **1988**, *332*, 332-334.
(6) Hansma, P. K.; Elings, V. B.; Marti, O.; Bracker, C. E. *Science* **1988**, *242*, 209-216.
(7) Worcester, D. L.; Kim, H. S.; Miller, R. G.; Bryant, P. J. *J. Vac. Sci. Technol. A* **1990**, *8*, 403-405.
(8) Patil, R.; Kim, S. J.; Smith, E.; Reneker, D.; Weisenhorn, A. L. *Polym. Comm.* **1990**, *31*, 455-457.
(9) Butt, H. J.; Downing, K. H.; Hansma, P. K. *Biophys. J.* **1990**, *58*, 1473-1480.
(10) Marti, O.; Ribi, H. O.; Drake, B.; Albrecht, T. R.; Quate, C. F.; Hansma, P. K. *Science* **1988**, *239*, 50-52.
(11) Meyer, E.; Howald, L.; Overney, R. M.; Heinzelmann, H.; Frommer, J.; Güntherodt, H.-J.; Wagner, T.; Schier, H.; Roth, S. *Nature* **1991**, *349*, 398-400.
(12) Weisenhorn, A. L.; Egger, M.; Ohnesorge, F.; Gould, S. A. C.; Heyn, S.-P.; Hansma, H. G.; Sinsheimer, R. L.; Gaub, H. E.; Hansma, P. K. *Langmuir* **1991**, *7*, 8-12.
(13) Hansma, H. G.; Gould, S. A. C.; Hansma, P. K.; Gaub, H. E.; Longo, M. L.; Zasadzinski, J. A. N. *Langmuir* **1991**, *7*, 1051-1054.
(14) For excellent reviews on Langmuir-Blodgett technique, see: (a) Kuhn, H.; Möbius, D.; Bücher, H. In *Physical Methods of Chemistry*; Weissberger, A., Rossiter, B., Eds.; Wiley: New York, 1972; Vol. 1, Part 3B. (b) Gaines, G. L., Jr. *Insoluble Monolayers at Liquid-Gas Interfaces*; Interscience: New York, 1966. (c) Roberts, G., Ed. *Langmuir-Blodgett Films*; Plenum Press: New York, 1990.
(15) See, for example: Sugi, M. *J. Mol. Electron.* **1985**, *1*, 3-17.

0002-7863/92/1514-7637$03.00/0

Table I. The Maximum Attractive Interaction Force of the Cantilever with the Sample[a]

sample	maximum attractive force (10^{-8} N) for cantilever k_i				roughness (nm)	
	k_1 = 0.06 N/m	k_2 = 0.12 N/m	k_3 = 0.38 N/m	k_4 = 0.58 N/m	$A < 100$ nm^2	$A < 1000$ nm^2
glass	1–4	1–6	1–8	30–60	6.7	8.3
glass + 1 LB layer	1–10	0.5–1	6–8	40–50	1.5	4.4
glass + 5 LB layers	5–10	0.3–0.5	2–8	50–60	0.8	1.3
glass + 25 LB layers	2–8	1–1.5	3–5	8–10	0.7	1.9

[a] The mean standard deviation for the given roughness values is 10%.

thicknesses for the LB multilayer structures were measured with the Philips APD1700 automated power X-ray diffractometer system using a copper Kα line (0.1542 nm), proportional detector, Ni filter, automatic divergence slit, and a tube voltage and current of 50 kV and 40 mA, respectively.

Atomic Force Microscope. A Nanoscope II (Digital Instruments, Inc., Santa Barbara, CA) AFM was used to image the sample surfaces. The scanner head A (0.7 μm scan range) was used for the imaging, but when the force was determined, head D (15 μm scan range) with better dynamics in the Z-range was applied. The 100 μm cantilever tip with a spring constant of k = 0.38 N/m proved to give the images with highest resolution. In addition, comparison of four different types of cantilevers is given in the results. The sample of ca. 5 × 5 mm^2 was adhered to a circular metal plate which was magnetically attached to the *xyz*-piezoscanner. Before the measurements were taken, the AFM was allowed to thermally stabilize at least 30 min after being switched on. The height mode was used to scan the surface. The system automatically keeps the force and hence the distance between the tip and the surface constant. The deflection of the cantilever is then detected with an optical level detection system.[16] As soft surfaces were involved, it was important to minimize the AFM contact force by tuning the setpoint voltage from its initial zero value to negative values even down to −4.5 V. The measuring unit was placed on a vibration-isolating table to eliminate external vibrational noise. In addition, high-pass filtering via both the electronics and software was used to cut off low-frequency noise. The low-pass filter was kept at its minimum value. Relatively high scanning speeds (10–30 lines/s) were found to be most suitable for scanning areas not larger than 100 × 100 nm^2. All the images (400 × 400 pixels) were measured in air.

Results

The attachment of the LB film monolayers deposited on the glass substrate was confirmed by X-ray diffraction. The small-angle diffraction plot showed several peaks, indicating a film structure with constant monolayer thickness of 2.36 ± 0.03 nm for Tb-TODA and 2.47 ± 0.05 nm for Cd-TODA, respectively. Compared with the theoretical length of the molecule and assuming an all-trans conformation, the hydrocarbon chains were found to be tilted about 16° and 7°, respectively, from the surface normal.

Four different types of triangular cantilevers microfabricated of a silicon wafer were tested in the AFM measurements. The longer ones are 200 μm long and the short ones are 100 μm long, and they also have different mass and thus different spring constants. These differences not only lead to varying interaction forces with the sample but also crucially affect the dynamic response of the imaging process. The optimization of these parameters is important when soft organic surfaces with nanometer-scale details are imaged. Table I summarizes the forces between the measured sample and the various cantilever tips. Referring to the cantilevers according to their spring constants k_i, cantilever k_1 (200 μm, narrow legs) was very unstable. It was difficult to determine images at all because the tip jumped off the sample surface relatively easily. The resolution for those images that we obtained was low. Cantilever k_2 (200 μm, wide legs) with the smallest interaction forces among the studied cantilevers seemed to be suitable for large-scale imaging (areas bigger than 200 nm^2). It was best suited for surfaces with large variations in vertical range, and the length and the big mass make it stable but simultaneously somewhat slow. We believe this mechanical slowness was the main reason for the fact that we could not reach molecular resolution with this cantilever. Cantilever k_4 (100 μm, wide legs) gave clearly the largest interaction forces, and it proved to be least suitable for LB film imaging. This cantilever modified the surface by generating holes in the LB films as well as enlargening the existing ones. The most stable images with the highest resolution could be measured with cantilever k_3 (100 μm, narrow legs). The interaction force between the tip and the sample surface could be easily controlled by the adjustment of the setpoint voltage. After force minimization the surface could be scanned with good dynamic response without destroying or modifying the surface. However, if a big force was chosen, the function of the tip started to duplicate that of cantilever k_4. Thus, one could even consider the possibility of etching the surface in a controlled manner. All the images shown in this study are taken with cantilever k_3.

Also given in Table I are the values of the roughness parameter for the studied surfaces. Independent of surface area, the tendency for a decreasing roughness with increasing number of LB layers is clear. The roughness for a monolayer when measuring areas correspond to molecular resolution ($A < 100$ nm^2) is 1.5 nm, which is more than 50% of the theoretical monolayer thickness of 2.6 nm. This may be the reason for the fact that no images with molecular resolution for a monolayer could be collected; the glass surface roughness was too dominating. However, high-resolution images could be measured for structures with five or more layers. This can be correlated to the pronouncely lowered roughness of the studied surface. It can be mentioned that the best-quality surfaces being studied showed surface roughness not more than 0.2 nm. Another point worth noting is that while the glass surface is almost as rough in 100 nm^2 scale as in 1 μm^2 areas, the roughness for the samples with LB layers increases independent of layer number when moving toward larger areas. This indicates that the smoothness of LB layers is locally good while different types of discontinuities increase the large-scale roughness. Obvious reasons for the large roughness may be inhomogeneous LB deposition, impurities in the substrate surface, etc.

Figure 1a shows a nonfiltered AFM surface plot of a 40 × 40 nm^2 glass substrate used as the LB film support. The two-dimensional fast Fourier transform (FFT) spectrum of the image is inset in the figure. As expected for an amorphous glass surface, no spots in the FFT spectrum indicating the periodicity or regularity of the surface are seen. The surface quality varied somewhat from one substrate to another, so Figure 1a represents a typical glass substrate surface. In Figure 1b (40 × 40 nm^2), one monolayer of Cd-TODA has been deposited on the glass substrate. Also here, the FFT spectrum inserted in the image confirms that the surface exhibits no order; the rough glass substrate still dominates the structure of the surface. The main difference between Figures 1a and 1b is the changed roughness value which is clearly smaller for the sample with one monolayer. It should be mentioned that although the same glass substrate has been used in Figures 1a and 1b the images do not represent locally identical areas simply because we are not able to refocus exactly on the same place after sample replacement, i.e. after LB film deposition. Because of the poor substrate quality, i.e. high roughness compared with the monolayer thickness, we, instead of further monolayer studies, report on the detailed measurements of LB multilayer structures.

Figure 2 shows an AFM image of a 85 × 85 nm^2 surface of a film consisting of 25 layers of Tb-TODA deposited at a constant surface pressure of 20 mN/m. Figure 2a is the surface plot of the raw data which already shows the ordered structure with parallel rows and height fluctuations in the scale range of 0–0.25 nm. The two-dimensional FFT spectrum of the image is inserted in the figure, and it reveals the periodic spacing of the main rows to be 1.35 ± 0.10 nm. The nearest-neighbor spacing along the

(16) Meyer, G.; Amer, N. M. *Appl. Phys. Lett.* **1990**, *56*, 2100–2101.

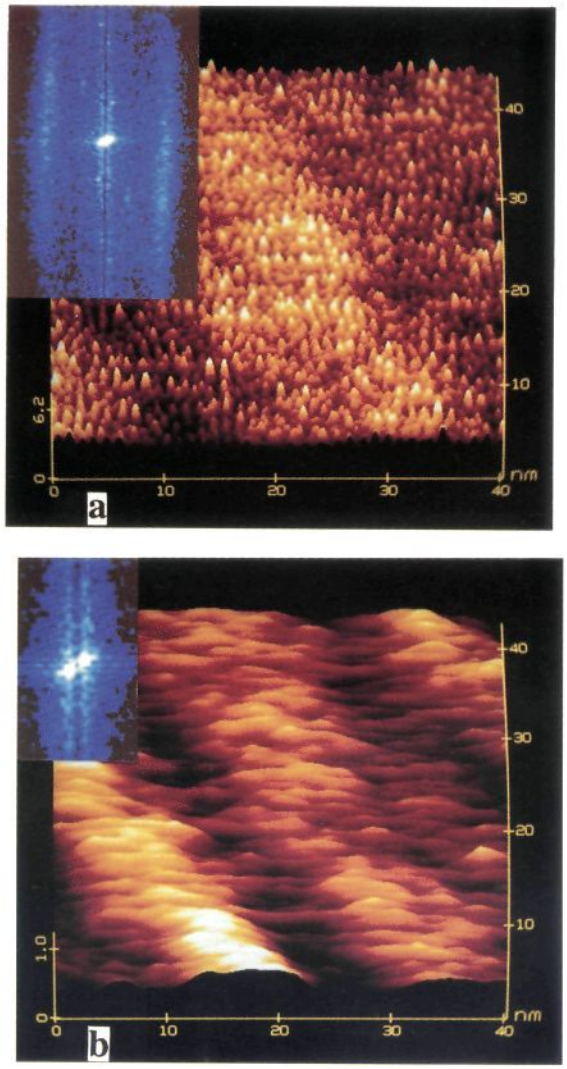

Figure 1. AFM images of a glass substrate (a) which is further coated with a Cd-TODA LB monolayer (b). The image size is 40 × 40 nm^2 and the characteristic FFT spectrum is inserted in both images. The black-to-white color scales (z-scale) are (a) 0–6.2 nm and (b) 0–1.0 nm.

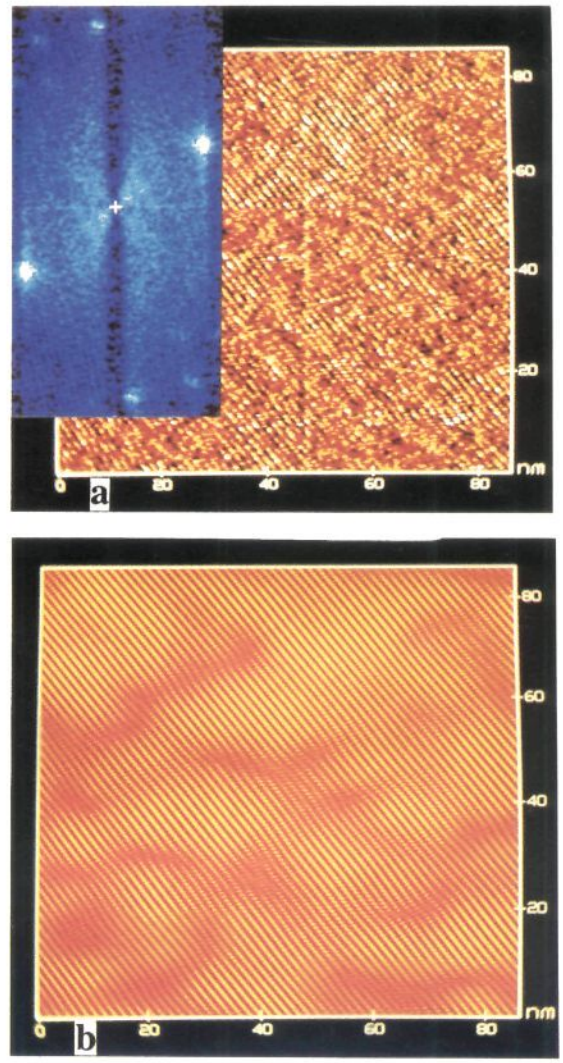

Figure 2. AFM image of a 25-layer Tb-TODA LB film. The scan area is 85 × 85 nm^2 and the black-to-white color scale (z-scale) is 0–0.25 nm. The image in (a) shows the raw scan of the surface with a specific 2-D FFT diffractogram inset in the image. The image in (b) illustrates the inverse-transformed top view of (a). For details see the text.

rows is 0.89 ± 0.03 nm. Figure 2b is the inverse-transformed and hence highly filtered version of Figure 1a derived by choosing the light spots in the FFT spectrum and then calculating the passband inverse FFT. The procedure leads to some resolution loss in the z-direction, but the filtered top view clearly exhibits the periodicity as well as the discontinuities existing in the surface. A typical dislocation, identical with that shown by Abraham,[17] is seen, for example, in the center of the image where a new line appears in the middle of the two lines coming obliquely down. Often, but not always, two similar types of dislocations but in reverse directions can be found, these two being not very distant from one another (a pair of dislocations).[17] Domain-like "islands" different in size, shape, and even periodicity appear in the image. The cross-section plots clearly showed the domain structure of the surface with domain-specific interrow spacings such as 1.26 and 1.58 nm. The dislocations found here always exist between the domains. However, the domain boundaries appear to be mainly smooth or to cause curves in the otherwise continuous and parallel rows. The vertical line crossing in the image almost in the center of Figure 2a may arise from some strong contrast in the substrate surface roughness. The exact explanation remains unknown.

Figure 3 illustrates the same sample as in Figure 2. Again, Figure 3a shows the raw image 20 × 20 nm^2 in size with its 2-D FFT spectrum inset in the figure. The appearance of several bright spots in the FFT diffractogram implies a highly ordered structure which is clearly revealed in the filtered surface plot (Figure 3b); the FFT spots containing the information on the periodicity are chosen and retained in the inverse Fourier transform. Compared with Figure 2, the smaller scan size gives more exact information about the fine structure of the surface. As is seen, the surface is a combination of subunits with single tops together with groups consisting of double and triple tops. Further, the structure along the main rows is not unity, but there seems to be a rotational degree of freedom around the z-axis of each individual subunit. This appears in the figure as a spiral-like structure along the main rows with alternating height from side to side within the rows. According to the FFT diffractogram, the separation of the "main" rows is 1.39 ± 0.12 nm (u-axis drawn in the image), however with an additional fine structure of 0.69 ± 0.03 nm and very weak 0.46 ± 0.02 nm spacings in an almost parallel direction with the u-axis. It is obvious from the image that these two periodicities more likely alternate locally than coexist simultaneously. This again refers to at least two different lattice subcells, of which the orthorhombic-like subcell is dominating. Further, instead of one, there are two main repeat spacings along these rows (v-axis): 0.44 ± 0.02 and 0.89 ± 0.03 nm. The cross section along the v-axis (Figure 3c) shows the pair-of-tops structure by the alternating amplitude

(17) Abraham, F. F. *Phys. Rep.* **1981**, *80*, 339–374.

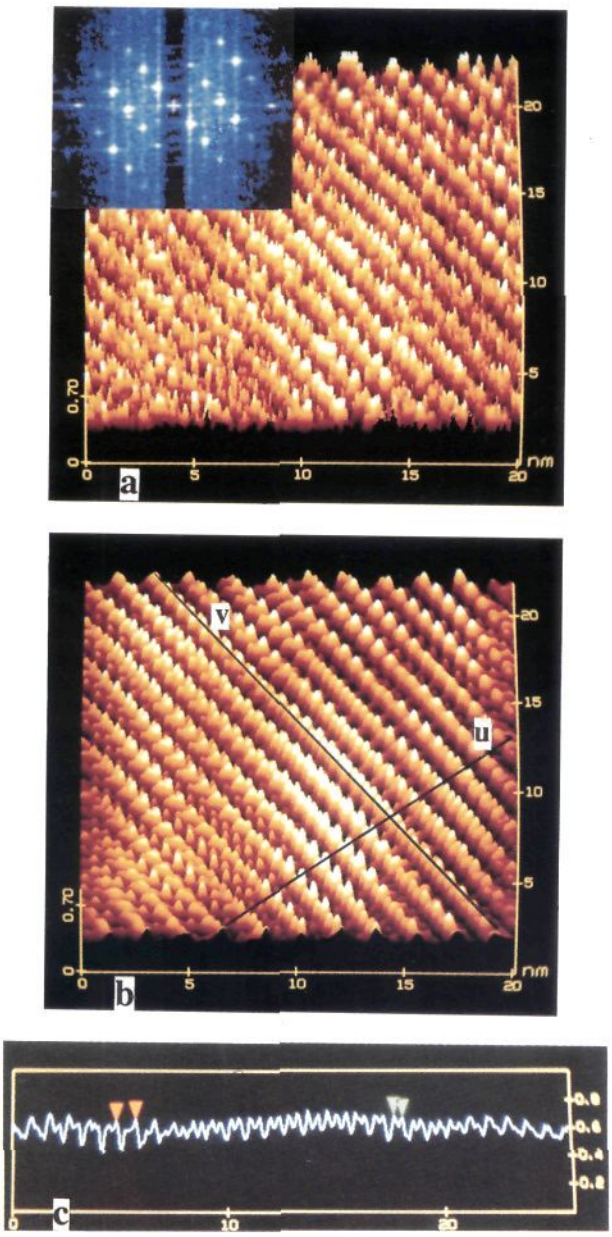

Figure 3. AFM image of a 25-layer Tb-TODA LB film with the scan area of 20 × 20 nm^2 and black-to-white z-scale of 0–0.5 nm. Image (a) corresponds to the original, nonfiltered data with its FFT spectrum. Image (b) presents the inverse-transformed surface plot of (*a*). The line profile in (c) shows the cross section of the surface along the v axis drawn in (b). The horizontal spacing between the drawn arrows on the left is 0.92 nm and that on the right is 0.44 nm.

between the tops. This indicates a binding of two nearest neighbors to exist along this direction. In comparison, the compression isotherm gave a mean molecular area of 0.210 ± 0.004 nm^2 for Tb-TODA at the deposition surface pressure chosen. This corresponds to an intermolecular distance of 0.516 ± 0.05 nm which is about 13% bigger than the obtained smallest nearest-neighbor spacings of the LB film structure shown in Figure 3. The increased packing density of the LB films together with the above explained alternations in height suggest that the packing during the deposition is changed so that the molecules on the glass substrate are arranged in two planes instead of the single plane packing which is typical for the Langmuir monolayer. This seems to be a result of the deposition process used together with the complex formation between the Tb^{3+} ions and the film molecules. Support for this model is given by the fact that the transfer ratio[18] especially for the first layers is higher than unity. If this is the case, the tilt angle should be somewhat smaller than that estimated for the X-ray data. However, we conclude that the light (=high) spots really image the molecules, strictly speaking the ends of the free hydrocarbon chains of the top layer.

To further investigate if AFM is unambiguously determining the different kinds of packing structures, we prepared a TODA LB film that was 5 layers thick and deposited from a $CdCl_2$ subphase at a constant surface pressure of 30 mN/m. Figure 4 shows the raw data with the characteristic FFT diffractogram and the inverse-filtered surface plot with a line profile through the imaged 10 × 10 nm^2 area. The differences compared with Figures 2 and 3 are obvious, which indicates an essentially different packing. All the molecules are now arranged in one plane. The lattice constants and the corresponding main axis directions in the FFT data suggested a crystal structure with nearest-neighbor spacings of 0.48 ± 0.03 nm (u-axis drawn in the image) and 0.51 ± 0.03 nm (v-axis) and an interaxis angle α of 68 ± 3°. The deviation of the lattice parameters, especially α, is considerable and cannot be explained to be due to a normal experimental error. Indeed, the cross section through the surface (Figure 4c) reveals the presence of areas or domains with specific packing densities and being occasionally separated by dislocations. The one-dimensional FFT spectrum shows the mean spacing along the drawn line to be 0.57 nm, while the arrows marked in the cross section shows specific nearest-neighbor spacings of 0.54 and 0.61 nm, respectively. The domain size compared with that for Figure 2 is now clearly smaller. The combination for the X-ray and AFM data indicates a triclinic subcell. The compression isotherm gave a mean molecular area of 0.190 ± 0.004 nm^2 at the deposition surface pressure. This result corresponds to an intermolecular spacing of 0.492 ± 0.005 nm and hence a good agreement with the AFM results, at least in the direction of the u-axis. The larger spacing in the v-axis direction may be related to the tilting of the CH_2 chains. The spacing of 0.51 nm together with simple geometry leads to a rough estimation for a tilt angle of 16°. This is about double that estimated from the X-ray diffraction data and hence refers to some other explanation for the tilt.

Discussion

Several facts support the claim that we really have been imaging the LB surface instead of the glass substrate or the AFM tip itself. While analyzing the image recorded for the pure glass no spots could be found in the FFT diffractogram which is typical for an amorphous surface. In the case of LB surfaces with 5 or more layers, an ordered structure with peculiar features could be found. The imaging of monolayers gave a somewhat smoother result than the glass surface, but still without signs of an ordered system. This suggests that the correlation between the amorphous substrate and the LB film orientation is lost after the deposition of several (≥5) monolayers. Varying lattice constants of the LB films with different counterions gave a good indication of the sensitivity of the AFM equipment. Further, the rotation of the sample during the measurement always rotated the corresponding image, including the defects obtained, respectively. This means that the system was not very sensitive to the geometry of the cantilever-tip measuring head used. We noticed that the use of a short and thin cantilever with spring constant k = 0.38 N/m gave images with best resolution and without damaging the film during scanning periods as long as several hours. The findings for the two-plane ordering suggest that the cantilever indeed imaged the top of the LB film structure without etching the surface or penetrating into the film. No harmful oscillations were recorded. The existence of such oscillations, however, was probably the reason for the failed tests experienced with cantilever k_1 of small spring constant. The use of cantilever k_4 resulted in harmful interactions between the tip and the LB layer, causing surface modification and destruction. It gives a good example of what may result under imaging conditions out of control.

(18) The transfer ratio is defined as the relation between the deposited substrate area and the corresponding change in monolayer area on the through surface. In an ideal case, the ratio equals 1.

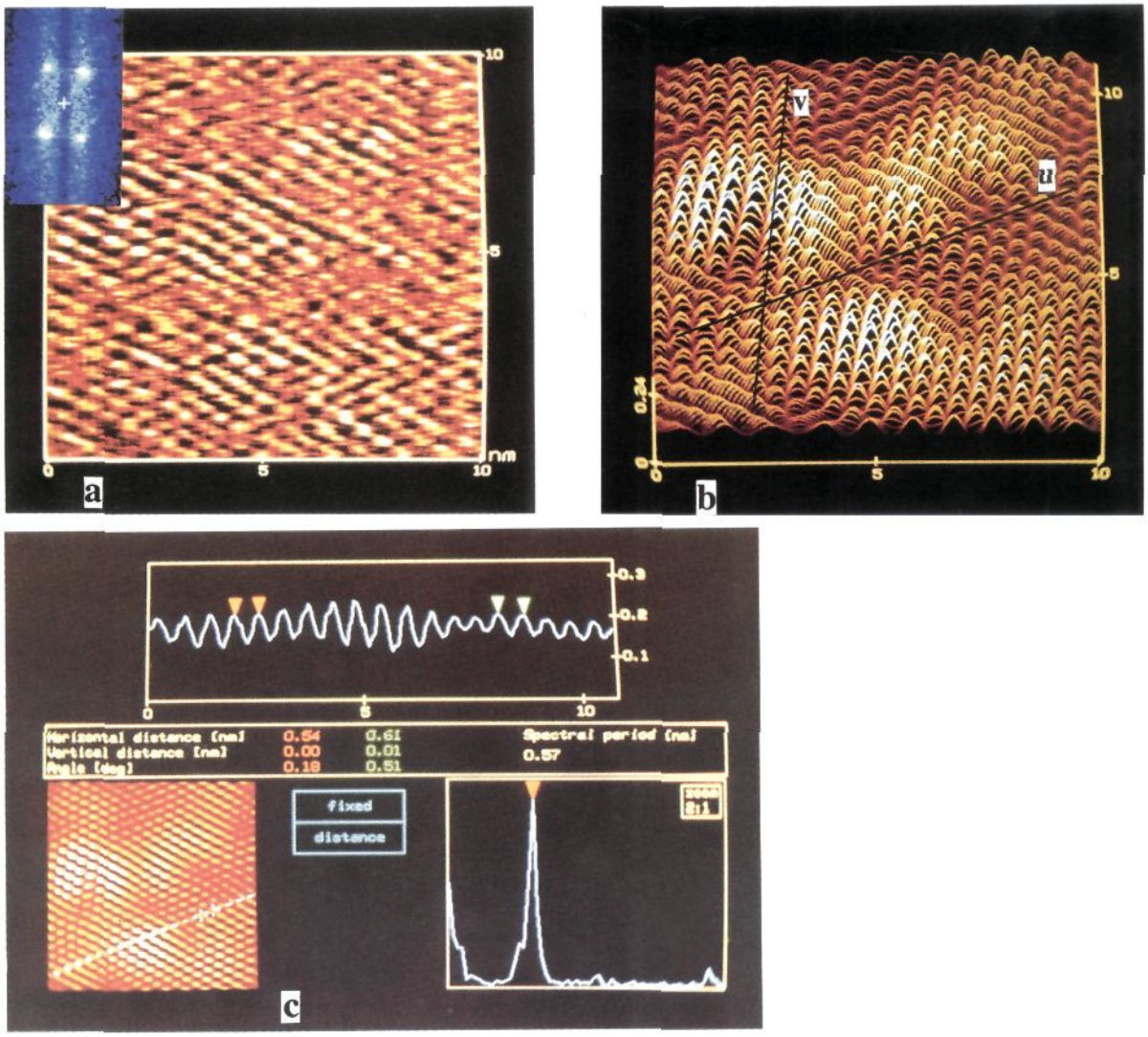

Figure 4. AFM image of a 5-layer CD-TODA LB film with the scan area of 10×10 nm^2 and black-to-white z-scale of 0–0.24 nm. Image (a) presents the raw data with the characteristic FFT diffractogram inserted. Image (b) shows the inverse-transformed line plot of (a). The line profile together with the one-dimensional FFT spectrum in (c) show the cross section of the surface along the line superimposed in the image. The horizontal spacings between the drawn arrows are 0.54 and 0.61 nm.

Meyer et al.[11] have used the AFM to study the Cd–arachidate (C20) LB films and reported repeat distances of 0.52 ± 0.03 and 0.47 ± 0.03 nm for a four-layer film, further suggesting an orthorhombic or monoclinic crystal structure. STM studies by Hörber et al.[19] gave intermolecular distances of 0.41 and 0.50 nm for a Cd–arachidate bilayer, indicating an orthorhombic unit cell. In that paper, a model of a liquid crystal-type structure reported by Nelson and Halperin[20,21] is suggested. The lattice spacings found in our work are in the same size range and seem thus to be reasonable. The findings suggest that the hydrocarbon chain with a trans-type double bond situated in the middle of the chain remains approximately straight. Spread on the subphase, the compression leads to a condensed monolayer with the mean molecular area almost equivalent to that of stearic acid. The intense X-ray diffraction peaks for the LB multilayer structures may also be taken as an indication of a homogeneous layer thickness. On the contrary, the Cd-TODA LB films show a variation of the periodic lattice spacing resembling the packing model reported by Safran et al.,[22] where the mismatch in size of the polar head group and the hydrocarbon chain leads to a nonuniform tilt angle for the hydrocarbon chains. The appearance of dislocations clearly indicates a similar type of liquid crystalline state as was reported by Hörber[19] as well as discussed earlier by Abraham.[17] The translational and long-range orientational order are disturbed by the dislocations, but the short-range order still remains. These findings hence give us an idea of the model being a combination of the two referred ones, where the distorted crystalline structure is additionally broken by dislocations. Support for this assumption is given by the findings of increasing roughness with increasing area under study. The reasons for the density fluctuations most probably arise from the interactions in the polar group region of the film. The presence of Cd ions in the subphase leads to the formation of Cd-TODA and Cd-$(TODA)_2$ complexes. A portion of nonbound TODA, however, remains associated due to the fact that at the used pH the monolayer is not fully ionized.[23] Among a wide range of studies concerning the influence of subphase on the monolayer formation, Neuman[24] has characterized the behavior of Ca–stearate monolayer as a function of pH. Our

(19) Hörber, J. K. H.; Lang, C. A.; Hänch, T. W.; Heckl, W. M.; Möhwald, H. *Chem. Phys. Lett.* **1988**, *145*, 151–158.
(20) Nelson, D. R.; Halperin, B. I. *Phys. Rev. B* **1979**, *19*, 2457–2484.
(21) Halperin, B. I.; Nelson, D. R. *Phys. Rev. Lett.* **1978**, *41*, 121–124.
(22) Safran, S. A.; Robbins, M. O.; Garoff, S. *Phys. Rev. A* **1986**, *33*, 2186–2189.
(23) See, for example: Ellis, J. W.; Pauley, J. L. *J. Colloid Sci.* **1964**, *19*, 755–764.
(24) Neuman, R. D. *J. Colloid Interface Sci.* **1975**, *53*, 161–171.

findings on the Cd-TODA multilayers suggest a similar kind of situation as presented by Neuman,[24] where the film prepared on the Ca subphase in the pH range 6.4–8.0 contained surface micelles. A possible alternative explanation for the inhomogeneous density arises from the fact that the stability of the monolayer was not ideal. This in turn led to relatively large oscillations in surface pressure during the deposition.

The situation is more complicated in the case of the Tb subphase. We believe that the coexistence of un-ionized TODA and Tb-TODA, Tb-$(TODA)_2$, and Tb-$(TODA)_3$ complexes results in the packing structure shown with more than one explicit subcell of symmetry present, but still maintaining reasonable values of intermolecular spacings. The existence of double complexes seems to be dominant. This is in accordance with our preliminary pH-dependent surface potential studies which suggest that the acid molecules on the Tb subphase are almost fully converted to the soap form at pH 5.7 used here. If one Tb ion binds two or three acid molecules this may lead to a lack of needed space in the polar region and thus results in the obtained packing into two planes. The degree of dissociation is largely ion dependent as is seen for example in the IR studies done by Aveyard et al.[25] According to our surface potential measurements the acid on the Cd subphase is only about 50% ionized at the operating pH.[26] Nevertheless, the packing differences are clear for the two ions used; the effect may not be purely ion dependent but also more generally pH dependent. A more comprehensive study of the pH-dependent salt effects on the monolayer properties will be given elsewhere.

Equivalent to the Cd-TODA multilayers, the characteristic properties of liquid crystalline phases exist in the Tb-TODA multilayers, however, with certain differences. The larger domain size suggests that the system is relatively close to the pure crystalline phase.[27] this is expected also from the compression isotherm, where a straight line with almost infinite slope is obtained within the surface pressure range of 10–40 mN/m. This relates to a low compressibility, and low fluctuations in density, which is characteristic for a single-phase system.[28] In contradiction with the mean molecular areas corresponding to the deposition surface pressure, the use of Tb instead of Cd seems to lead to a closer-packed crystal structure on the LB film. These findings about the change in packing type during the deposition process were discussed earlier. The packing density has certain analogy with the paper of Abraham et al.,[29] who showed that the presence of trivalent subphase ions[30] leads to a very rigid film. Anyway, the results revealing the clear differences in the packing modes between Cd-TODA and Tb-TODA LB films strongly support the idea presented by Helm et al.[31] and theoretically analyzed by Andelman et al.[32,33] that electrostatic interactions and especially the ionic strength and pH of the subphase have a crucial effect on the monolayer properties.

Conclusions

In conclusion we have demonstrated the ability of the AFM to image LB films at molecular resolution and to distinguish between not only packing symmetries but also local properties within one phase. The extreme resolution was achieved by comparing four different types of cantilevers and then choosing the one being most suitable for this study. When investigating well-organized systems, the FFT algorithm provided a useful tool for image analysis and lattice parameter detection. It nevertheless represents a relatively extensive filtering technique. By overcoming the problems concerning the acoustic noise it however seems possible in the near future to further approach the atomic scale resolution. Moreover an alternative choice of substrate may enable us to investigate a single LB layer.

Acknowledgment. The authors acknowledge useful discussions with Prof. M. Hotokka and Mr. M. Linden and the AFM instrument installation by T. Bergman and R. Yli-untinen. We also thank Kamera-Aitta for excellent service on photograph development. The work was financed by the Technology Development Centre, TEKES, Finland.

(25) Aveyard, R.; Binks, B. P.; Carr, N.; Cross, A. W. *Thin Solid Films* **1990**, *188*, 361–373.
(26) For comparison, see: Petrov, J. G.; Kuleff, I.; Platikanov, D. *J. Colloid Interface Sci.* **1982**, *88*, 29–35.
(27) Fischer, A.; Sackmann, E. *J. Colloid Interface Sci.* **1986**, *112*, 1–14.
(28) Lee, A. G. *Prog. Mol. Biol. Biophys.* **1975**, *29*, 5–56.
(29) Abraham, B. M.; Ketterson, J. B.; Miyano, K.; Kueny, A. *J. Chem. Phys.* **1981**, *75*, 3137–3141.
(30) The comparisons were made for Al^{3+}, Fe^{3+}, Ca^{2+}, and Mg^{2+} ions.
(31) Helm, C. A.; Laxhuber, L.; Lösche, M.; Möhwald, H. *Colloid Polym. Sci.* **1986**, *264*, 46–55.
(32) Andelman, D.; Broçhard, F.; Joanny, J.-F. *J. Chem. Phys.* **1987**, *86*, 3673–3681.
(33) Andelman, D.; Broçhard, F.; Joanny, J.-F. *Proc. Natl. Acad. Sci. U.S.A.* **1987**, *84*, 4717–4718.